Applied Surface Science 353 (2015) 820–828

Contents lists available at ScienceDirect

Applied Surface Science

journal homepage: www.elsevier.com/locate/apsusc

A theoretical view of 1,3-butadiene selective hydrogenation toward *cis*-2-butene on Pd—Ni layered catalyst

Guillermina Gómez, Patricia G. Belelli*, Gabriela F. Cabeza, Norberto J. Castellani

Grupo de Materiales y Sistemas Catalíticos, Departamento de Física (IFISUR-CONICET), Universidad Nacional del Sur, Av. Alem 1253, Bahía Blanca B8000CP, Argentina

ARTICLE INFO

Article history:
Received 28 May 2015
Received in revised form 19 June 2015
Accepted 19 June 2015
Available online 25 June 2015

Keywords:
1,3-Butadiene
Isomerization
Pd—Ni surface
Periodic DFT

ABSTRACT

The production of *cis*-2-butene (*cis*-2B) on Pd/Ni(1 1 1) bimetallic model was evaluated considering two possible reactions: through the hydrogenation of 1,3-butadiene (13BD) adsorbed on a *cis*-geometry site and through the isomerization of *trans*-2-butene (*trans*-2B). For that purpose, density functional theory (DFT) calculations were performed following the corresponding Horiuti–Polanyi mechanisms. In the hydrogenation, two competitive pathways produce *cis*-2B and *trans*-2B from 13BD species adsorbed on di-π-*cis* and 1,2,3,4-tetra-σ sites, respectively. The *cis*-2B is obtained with smaller energy requirements than the *trans*-2B isomer in spite of the adsorption of 13BD on the di-π-*cis* site is 0.10 eV less stable than on the 1,2,3,4-tetra-σ site. On the other hand, the *trans*-2B previously formed could be isomerized to *cis*-2B, and vice versa, trough the 2-butyl intermediates, but the elevated energetic barriers to hydrogenate/dehydrogenate both 2B isomers would avoid these processes. In fact, the dehydrogenation reaction is the limiting step of the isomerization reaction. From these results, we infer that on the Pd/Ni(1 1 1) surface the *cis*-2B isomer is easier to be formed via the 13BD hydrogenation on the di-π-*cis* site than via the *trans*/*cis* isomerization of 2B.

1. Introduction

The conversion of alkenes by transition metals (TM) is one of the most studied catalytic reactions; nevertheless, some main topics still remain unresolved [1–3]. Specifically, it is not clear yet what controls selectivity toward the formation of *cis*- or *trans*-olefins [4]. This issue is of interest in the food industry to reduce the *trans*-fatty acids production during the partial hydrogenation of natural oils to edible fats. The evidence of cardiovascular health risks caused by *trans*-fatty acids is one of the most significant efforts to improve the selectivity toward the *cis*-formation [5]. In particular, the selective hydrogenation of 1,3-butadiene (13BD) is considered as a reaction test for probing the activity and electronic structure of metal catalysts.

During the development of a chemical reaction of petrochemical interest, a lot of steps take place and some of them yield undesired products by the so-called side reactions. In particular and according to the Horiuti–Polanyi mechanism, during the 13BD partial hydrogenation (see Scheme 1) their conjugated C=C double bonds can be hydrogenated through two different routes: 1,2-addition to form 1-butene (1B) and 1,4-addition to form 2-butene (2B), as primary products. Because 13BD has *trans*- and *cis*-isomers, the hydrogenation will produce either the *trans*- or the *cis*-2B products. The ulterior isomerization of any of latter can be considered as a side reaction if only one of them is desired. Moreover, all the butene products can be converted to saturated species upon further hydrogenation, which can be considered as another undesired reaction.

Regarding the TM used as catalyst, the experiments show that Pd provides higher selectivity in the 13BD partial hydrogenation to 1B compared with Pt [6,7]. Initially, it was thought that the selective partial hydrogenation on the surface of these systems could be explained from the difference in desorption energies between the 13BD and butene [1]. Subsequent studies revealed that the nature of bonding on metal surfaces, i.e., di-π bonding on Pd and di-σ bonding on Pt, also strongly affects the selectivity in 13BD hydrogenation toward 1B instead of butane [8,9]. More recently, Katano et al. [10] findings indicate that the hydrogenation of π-bonded 13BD on Pd(1 1 0) shows significant selectivity to butenes. In particular, the high hydrogenation activity of weakly π-bonded 13BD, combined with the instability of butenes produced at the reaction temperature, are the main reasons for the high selectivity on Pd(1 1 0) [11].

* Corresponding author. Tel.: +54 291 4595141; fax: +54 291 4595142.
E-mail address: patricia.belelli@uns.edu.ar (P.G. Belelli).

http://dx.doi.org/10.1016/j.apsusc.2015.06.127
0169-4332/

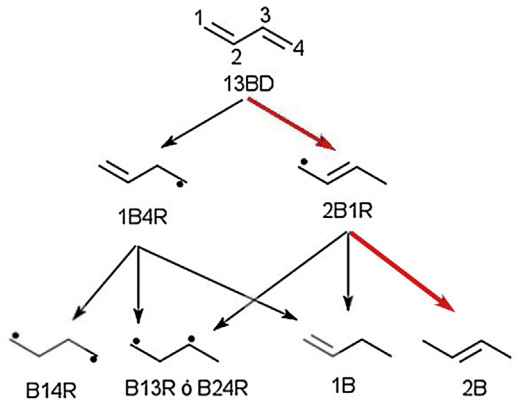

Scheme 1. Schematic representation of Horiuti–Polanyi mechanism for 13BD partial hydrogenation. Dot notation indicates radical and diradical species.

It is a well known fact that the catalytic properties of bimetallic catalysts usually exceed the properties of one of the metal components. Some experimental studies reported the origin of this interesting effect using model surfaces [12–14]. One of the governing factors is the average metal–metal bond length, which is different to those of the corresponding pure metals and produces a strain effect. The changes in orbital overlap are accompanied by modifications of the electronic structure [15,16]. Besides the electronic effects, the activity and selectivity of bimetallic catalysts can be improved due to the geometric effect at the surface, i.e., the second metal may block sites of the first metal on the surface and consequently the average size and composition of the active sites can be varied [17]. This is the case for the bimetallic Pt/Ni system, where the Pt enriched surface over a Ni substrate is very active for low temperature hydrogenation reactions [133–144, 155, 166, [18]].

In order to improve the sunflower oil hydrogenation, different bimetallic Pt/Ni catalysts supported on mesoporous silica were recently synthetized [19]. Experimental results show that the addition of Ni on Pt/SiO_2 catalyst produces a significant drop in the *trans*-formation, compared to the corresponding Pt monometallic catalyst. This behavior is explained trough the electronic and geometric effects generated by the incorporation of the second metal on the surface. In another case, the restructuring of the Pd/Ni(1 1 0) surface was considered to explain the catalytic activity increase of the 13BD hydrogenation, when palladium coverage exceeds 0.5 mL [20]. Recently, the 13BD selective hydrogenation to 1B was investigated theoretically and experimentally over a Ni/Pd(1 1 1) bimetallic catalyst with good correlation between both points of view [21].

The theoretical study of a bimetallic TM catalyst for hydrogenation was already addressed previously by us [22]. Specifically, the partial hydrogenation of 13BD to 1B, 2B and butan-1,3-diyl (B13R) on Pd/Ni(1 1 1) and Pd_3/Ni(1 1 1) bimetallic surfaces was investigated using a periodic method. According to the Horiuti–Polanyi mechanism, the overall process is exothermic on the Pd/Ni(1 1 1) system and endothermic on Pd_3/Ni(1 1 1). Concerning the Pd/Ni(1 1 1) catalyst model, the intermediates present more favorable adsorptions and lower activation barriers than Pd_3/Ni(1 1 1). The products would be mainly the butene isomers, with a slightly more selectivity toward 2B, in contrast to the pure Pd(1 1 1) surface [23], and in agreement with experimental data [8,24–28]. Nevertheless, it is well known that 13BD is preferentially adsorbed with *trans*-geometry of 1,2,3,4-tetra-σ configuration on several transition metals [29–31], and for this reason the *trans*-2B isomer was always obtained. But there are opened questions about what happens with the *cis*-2B isomer and how it is formed.

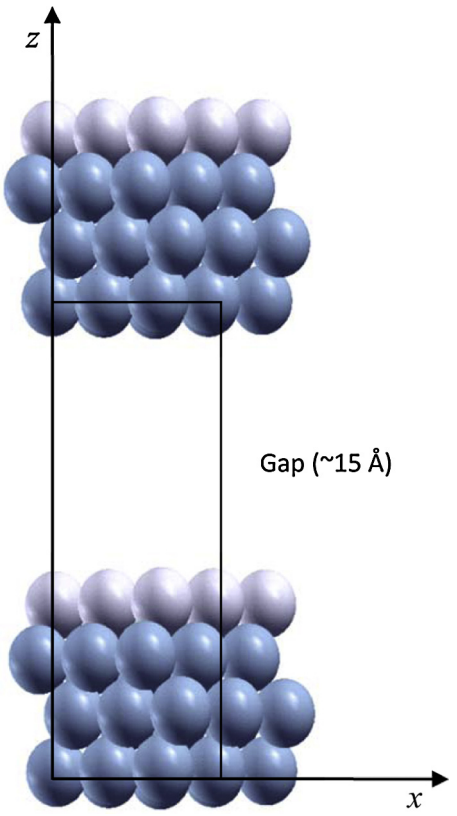

Fig. 1. Side view of the slab used as model for the Pd/Ni(1 1 1) bimetallic surface. White and gray balls correspond to Pd and Ni atoms, respectively. (For the interpretation of the references to color in this figure legend, the reader is referred to the Web version of this article.)

The aim of this work is to study the *cis*-2B production during the 13BD partial hydrogenation on a multilayered Pd/Ni(1 1 1) surface following two possible reaction paths: (1) through the partial hydrogenation of 13BD adsorbed with *cis*-geometry, in a di-π-*cis* configuration, or (2) through the isomerization of *trans*-2B, previously formed from the partial hydrogenation of 13BD adsorbed with *trans*-geometry.

2. Computational details and surface models

Total energy DFT calculations reported in this work were performed using VASP code [32–34] and the projector augmented-wave method (PAW) developed by Blöch was applied [35]. The PAWs of ten valence electrons for Ni ($3d^8 4s^2$) and for Pd ($4d^{10}$) were considered. For the exchange–correlation effects we adopted the generalized gradient approximation (GGA) using the proposed Perdew–Wang (PW91) functional [36,37]. The kinetic energy cutoff for the plane wave expansion of the electronic wavefunction was 450 eV. A $(3 \times 3 \times 1)$ Monkhorst–Pack k-point mesh was used [38]. The convergence of the k-point mesh was checked until the energy had converged with a precision better than 1 meV/atom. The Methfessel–Paxton technique [39] with a smearing factor of 0.2 eV was applied to determine how the partial occupancies are set for each one-electron wave function electronic levels. The criterion for the self-consistent convergence of the total energy was 0.1 meV. The calculations were performed at the spin polarized level.

A FCC stacking layered structure was assumed. The slab representing the (1 1 1) metallic surface was constructed containing four layers of atoms (one Pd layer over three Ni layers) separated in the normal direction by a vacuum region (Fig. 1). This gap was optimized and a value of ~15 Å was adequate to avoid the interaction

between slabs. The structural, electronic and magnetic properties of Pd/Ni(1 1 1) was previously analyzed considering the ferromagnetic condition acquired by the Pd overlayer epitaxially deposited on the Ni(1 1 1) surface [40]. The Pd—Pd interatomic distances in the first layer were optimized to 2.57 Å. The geometries of adsorbates together with the two uppermost layers of the surface were fully optimized.

The transition states (TS) and the activation energy barriers (ΔE_{TS}) were determined using the Nudged Elastic Band Method (NEB) [41]. This was performed until a negligible value of the forces was achieved. The transition states were validated by checking the full vibrational frequency analysis achieved by calculating the Hessian matrix, followed by a diagonalization procedure to obtain the eigenmodes. All the corresponding transition states had only one negative force constant. Afterward, the eigenvector associated with this negative force constant was related to the reaction pathway considered. This procedure allowed us to obtain accurate transition states and activation barriers.

As it will be seen in Section 3, the red arrows of Schemes 1 and 2 and their corresponding explanations, given in the successive paragraphs, describe the routes used in the NEB calculation. From a technical point of view, a systematic searching of the minimal energy configuration was performed for each situation. For example, in the case of C_4H_x (x = 6 or 7) species co-adsorbed with a H atom, several geometrical configurations neighboring the C atom to be hydrogenated were evaluated; but only the most stable was selected to build the reaction pathway. These minimal energy configurations were used as starting and end points in the NEB calculation.

Energy profiles associated with the reaction pathways were calculated assuming certain energy as reference. Specifically, to obtain the relative hydrogenation energy, E_{HYDROG_rel}, the sum of energies of isolated 13BD and H_2 molecules in gas phase was taken as reference. E_{HYDROG_rel} was calculated according to the equation:

$$E_{HYDROG\_rel} = E_{C_4H_x/surf} + (8-x)E_{H/surf} - (9-x)E_{surf} - E_{C_4H_6(g)} - E_{H_2(g)} \quad (1)$$

where C_4H_x corresponds to 13BD, to 13BD in co-adsorption with H, to one of the possible intermediates as well as to the latter in co-adsorption with another H; $E_{H/surf}$ is the adsorption energy of an isolated hydrogen atom and E_{surf} is the energy of the bare surface; $E_{C_4H_6(g)}$ and $E_{H_2(g)}$ are the energies of 13BD and H_2 molecules in gas phase respectively; finally, x is the amount of H atoms in the reaction (x = 6, 7, 8).

In the case of the isomerization reaction the corresponding relative energy, E_{ISOM_rel}, was calculated with respect to the sum of energies of isolated *trans*-2B and H_2 molecules in gas phase, $E_{C_4H_8(g)}$ and $E_{C_4H_8(g)}$, respectively:

$$E_{ISOM\_rel} = E_{C_4H_x/surf} + (9-x)E_{H/surf} - (10-x)E_{surf} - E_{C_4H_8(g)} - 1/2E_{H_2(g)} \quad (2)$$

where C_4H_x corresponds to 2B isomers and to 2B in co-adsorption with H and x is the amount of H atoms in the reaction (x = 8, 9). For both reactions, negative values indicate the exothermicity of the reaction process. Non Zero Point Energy (ZPE) corrections were made because the ZPE contributions to reaction energies and the activation energies were below 0.01 eV.

3. Results and discussion

As it was previously mentioned, the *cis*-2B product could be obtained from the 13BD partial hydrogenation or from the isomerization reaction of *trans*-2B, with the last one being previously formed from the 13BD partial hydrogenation. It is important to emphasize that both hydrogenation and isomerization reactions are expected to occur during the experimental reaction. The 13BD geometry is always associated with a *trans*-isomer because it is more stable than that for the *cis*-isomer in the gas phase. For this reason, it is expected that the *trans*-2B would be the more favorable 2B product.

The 13BD partial hydrogenation to obtain 2B isomers and the *cis*/*trans*-2B isomerization were analyzed following the mechanisms proposed by Horiuti–Polanyi [42,43]. In Scheme 1, the whole Horiuti–Polanyi mechanism for hydrogenation is displayed, where the addition of an H atom into one of the C=C double bonds of 13BD produces two C_4H_7 intermediates: 1-buten-4-yl (CH_2=$CHCH_2CH_2$•, 1B4R) and 2-buten-1-yl (CH_2•CH=$CHCH_3$, 2B1R), when H atom is added on C_2 (or C_3) and C_1 (or C_4), respectively. The subsequent incorporation of another H atom yields the C_4H_6 products: 1-butene (1B), 2-butene (2B) and the diradicals butan-1,3-diyl (B13R) and butan-1,4-diyl (B14R). All these steps were studied in our recently published paper [22], but in the present work only the pathway forming the 2B product, through the 2B1R intermediate, will be considered (red arrows in Scheme 1). This choice was taken considering that this pathway constitutes the only one to obtain the 2B product as well as that the 2B1R intermediate has a higher stability than the 1B4R one, due to its allylic character [22]. Thus, the hydrogenation reaction will occur through a 1,4-addition of H. The radical (1B4R, 2B1R) and diradicals (B14R, B13R) species of different intermediates (C_4H_7 and C_4H_8) are indicated in Scheme 1 using dot notation.

In the Horiuti–Polanyi isomerization mechanism [42], the C_4H_9 moiety is formed through the insertion of a H atom into the C=C double bond of one the C_4H_8 species and an ulterior dehydrogenation produces the other C_4H_8 isomer. In Scheme 2, the H atom added to the *trans*-2B isomer produces the *trans*-2-butyl partial hydrogenated intermediate. The easy rotation around the central C—C simple bond forms the *cis*-2-butyl. The following dehydrogenation of the C atom previously hydrogenated forms the *cis*-2B isomer. In this simple scheme, the selectivity is explained by the removal of a hydrogen atom from the β-position of the alkyl intermediate.

3.1. 13BD hydrogenation

In our earlier work, the 1,2,3,4-tetra-σ site was obtained as the preferable adsorption mode of 13BD on Pd/Ni(1 1 1) surface, while the di-π-*cis* site was only 0.1 eV less stable [22]. In these two sites the 13BD molecule has different geometry: on 1,2,3,4-tetra-σ site the diene is adsorbed with *trans*-geometry (see Fig. 2a), while on di-π-*cis* site the 13BD has *cis*-geometry (see Fig. 3a). Therefore, it is largely expected that *cis*-2B and *trans*-2B yielding, obtained as products of 13BD partial hydrogenation, would depend on the initial 13BD geometry on the adsorption site. Comparing the adsorption energies for both 13BD geometries on Pd/Ni(1 1 1) with respect to Pd(1 1 1) [29], we observed that di-π-*cis* site is ~0.20 eV favored in our Pd/Ni(1 1 1) model [31]. This suggest a higher proportion of 13BD adsorbed on this site of Pd/Ni(1 1 1), compared with Pd(1 1 1).

Firstly, the partial hydrogenation of 13BD adsorbed on 1,2,3,4-tetra-σ and di-π-*cis* of Pd/Ni(1 1 1) catalyst through 2B1R intermediate to form *trans*-2B and *cis*-2B, respectively, were evaluated. In Figs. 2 and 3 the optimized structures achieved along the whole reaction path are shown, from the adsorbed 13BD to the final products *cis*- and *trans*-2B, respectively.

In addition, the most important geometrical parameters of 13BD, 2B1R and *cis*/*trans*-2B species adsorbed on Pd/Ni(1 1 1), and their respective relative energies (E_{HYDROG_rel}) are summarized in Table 1. The E_{rel} values indicate the slightly high stability of 13BD adsorbed on 1,2,3,4-tetra-σ with respect to di-π-*cis* sites, as it was previously mentioned. Their energy difference can be associated

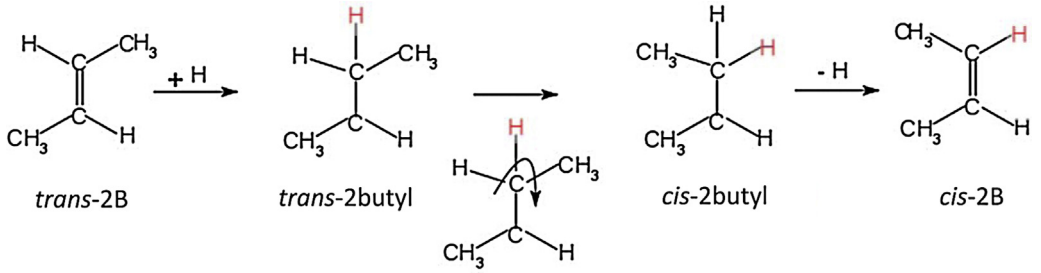

Scheme 2. Schematic representation of Horiuti–Polanyi mechanism for *trans*-2B isomerization. The curved arrow indicates the easy rotation around the central C—C simple bond of the *trans*-2butyl partial hydrogenated intermediate to form the *cis*-2butyl.

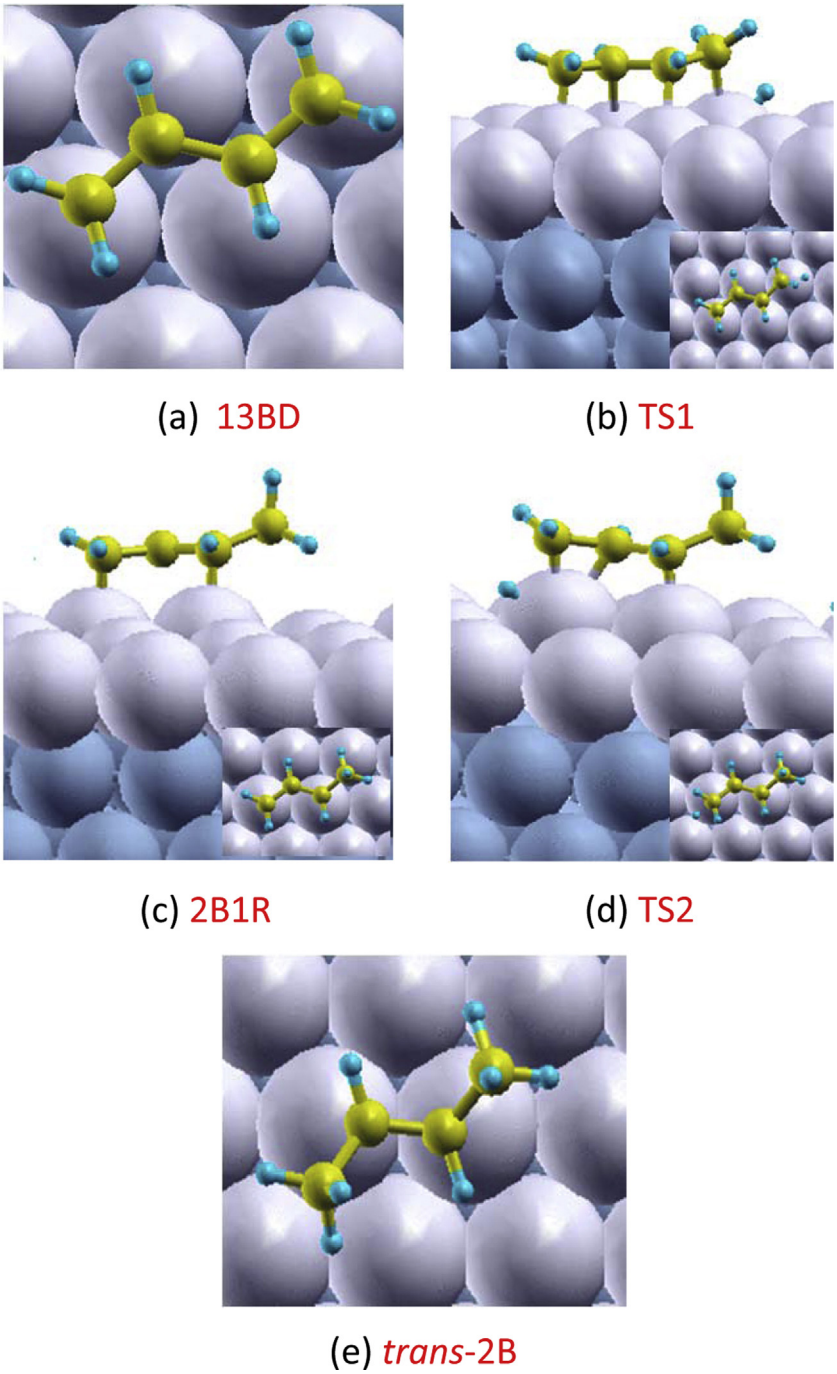

Fig. 2. Optimized geometries of species involved in the reaction path of 13BD partial hydrogenation on Pd/Ni(1 1 1) surface, to obtain the *trans*-2B product: (a) 13BD adsorbed on 1,2,3,4-tetra-σ site, (b) transition state 1 (TS1), (c) 2B1R, (d) transition state 2 (TS2) and (e) *trans*-2B.

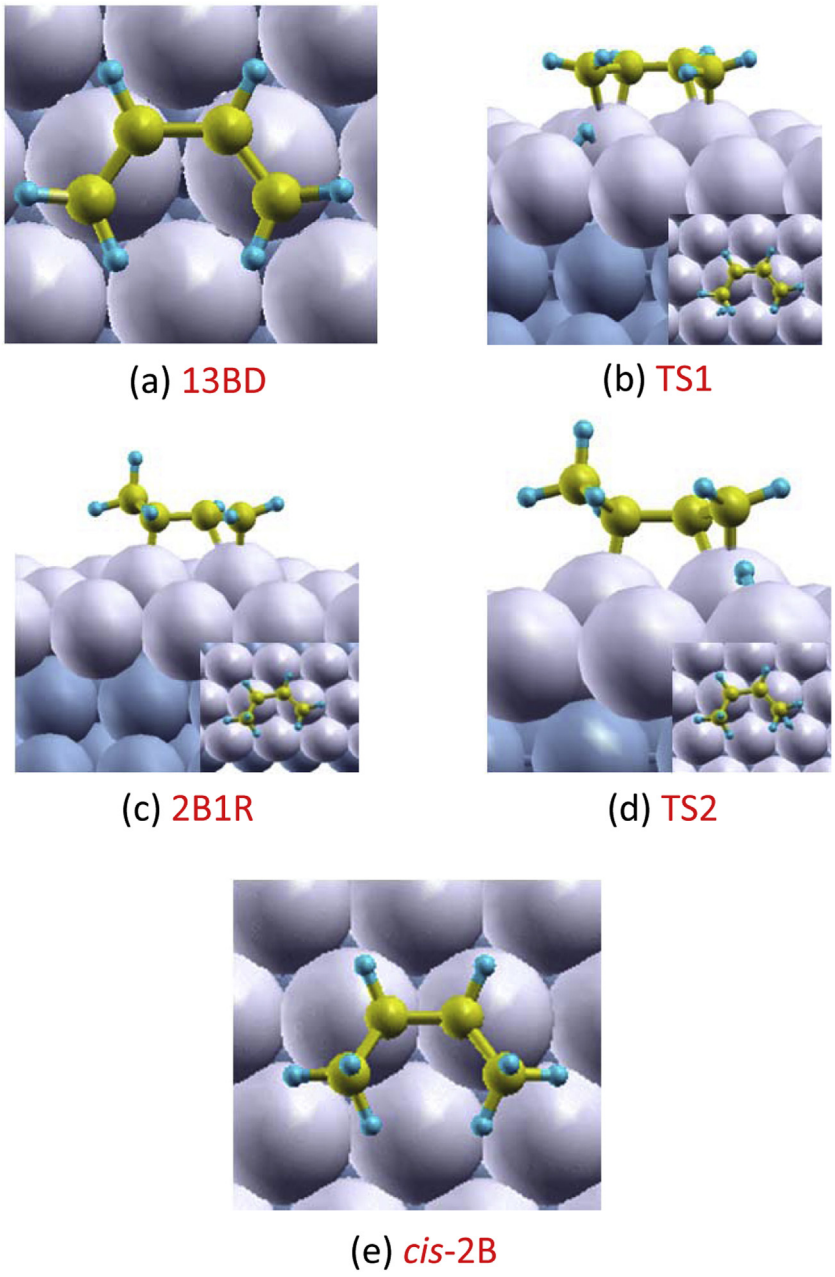

Fig. 3. Optimized geometries of species involved in the reaction path of 13BD partial hydrogenation on Pd/Ni(1 1 1) surface, to obtain the *cis*-2B product: (a) 13BD adsorbed on di-π-*cis* site, (b) transition state 1 (TS1), (c) 2B1R, (d) transition state 2 (TS2) and (e) *cis*-2B.

Table 1
Relative energies ($E_{HYDROG.rel}$), in eV, and more relevant bond distances, in Å, of the involved species in the 13BD hydrogenation on Pd/Ni(1 1 1) surface.

Product	*trans*-2B							
Species	$E_{HYDROG.rel}$	Pd—C_1	Pd—C_2	Pd—C_3	Pd—C_4	C_1—C_2	C_2—C_3	C_3—C_4
13BD	−1.04	2.16	2.34	2.43	2.16	1.43	1.43	1.43
13BD + H	−0.80	2.20	2.55	2.45	2.18	1.42	1.43	1.42
trans-2B1R	−1.35	2.14	2.58	2.20	3.22	1.43	1.42	1.51
trans-2B1R + H	−1.34	2.13	2.43	2.10	3.05	1.41	1.44	1.51
trans-2B	−1.42	3.14	2.22	2.23	3.16	1.50	1.40	1.51
Product	*cis*-2B							
Species	$E_{HYDROG.rel}$	Pd—C_1	Pd—C_2	Pd—C_3	Pd—C_4	C_1—C_2	C_2—C_3	C_3—C_4
13BD	−0.95	2.20	2.28	2.27	2.21	1.41	1.46	1.41
13BD + H	−0.75	2.23	2.29	2.28	2.21	1.40	1.46	1.41
cis-2B1R	−1.43	2.15	2.30	2.12	2.96	1.42	1.45	1.51
cis-2B1R + H	−1.30	2.14	2.34	2.11	2.95	1.42	1.45	1.51
cis-2B	−1.32	3.18	2.24	2.25	3.20	1.50	1.40	1.50

Table 2
Transition state barriers (ΔE_{TS}), in eV, and more relevant bond distances, in Å, of the intermediate and H co-adsorbed species and TS geometries in the 13BD hydrogenation on Pd/Ni(1 1 1) surface.

Products	*cis*-2B				*trans*-2B			
Species	ΔE_{TS}	Pd—H	C—H	Pd—C	ΔE_{TS}	Pd—H	C—H	Pd—C
13BD + H	–	3.06	2.95	2.23	–	1.87	2.57	2.18
13BD + H → 2B1R (**TS1**)	0.47	1.87	1.64	2.45	0.65	1.63	1.65	2.38
2B1R + H	–	2.98	3.47	2.14	–	1.79	2.78	2.13
2B1R + H → 2B (**TS2**)	0.51	1.76	1.58	2.29	0.60	1.66	1.59	2.24

with the surface interactions: in the first case, both C terminal atoms are more strongly linked with Pd than the central ones, having all C—C bonds the same lengths. For 13BD adsorbed on di-π-*cis* site, the C atoms are slightly farther away from the surface and the C=C double bonds are less lengthened. On the other hand, the 2B1R intermediates have two different geometries depending on the initial 13BD adsorption site (see Figs. 2c and 3c). Notice that the *cis*-2B1R intermediate has a higher stability than *trans*-2B1R. This fact could be related with the shorter Pd—C bonds, making the *cis*-2B1R radical slightly more activated than the *trans*-2B1R one. Besides, it is remarkable that the *trans*-2B has a more suitable geometry to adsorb on an *fcc* surface than the *cis*-2B, with the former product giving the shorter Pd—C distances. This feature is reflected in their respective E_{rel} values.

The geometry of the transition states (TS), basically established by a three centers structure (Pd—C—H), is formed when the co-adsorbed H atom begins to bind with the C atom of the 13BD, whereas at the same time the Pd—H and Pd—C bonds begin to be broken. In Table 2, these three distances of transition state geometries and their transition state energies (ΔE_{TS}) are presented. The Pd—C distance and the C—H and Pd—H bonds of TSs are longer and more shorten, respectively, than those of the corresponding co-adsorbed species (13BD + H for TS1 and 2B1R + H for TS2). Conversely, the Pd—H distances are shortened in TS geometries because the H atom adsorbed in the *fcc* hollow site moves away from two adjacent Pd atoms, approaching to the Pd atom where the C is linked. In both reaction paths, the H atom is added to a primary C atom, provoking significant geometrical transformations on the 13BD and 2B1R species because the C atom changes its hybridization from sp^2 to sp^3. In spite of this situation for both pathways, the TS1 geometries have no extremely enlarged Pd—C distances and retain the planarity (see Fig. 2b and 3b). For the second transition states TS2, a similar behavior was observed (see Fig. 2d and 3d). These features indicate the presence of the early transition state geometries according to the Hammond Postulate [44].

In Fig. 4, the 13BD hydrogenation energy profiles on 1,2,3,4-tetra-σ and di-π-*cis* active sites of Pd/Ni(1 1 1) are shown. The optimized geometries of different species and the transition states (TS1 and TS2) considered for both adsorption structures of 13BD correspond to those previously shown in pictures of Figs. 2 and 3. In the first and second steps of corresponding reaction pathways, the 13BD and H species are independently adsorbed and co-adsorbed on the metallic surface, respectively. The co-adsorption processes require approximately 0.2 eV, which is in agreement with previous values reported by other authors [23,45,46]. In general, the co-adsorptions produce instability with respect to the species independently adsorbed (see Table 1).

The production of the 2B1R intermediates (Figs. 2c and 3c) is a process highly favored thermodynamically with respect to the co-adsorbed species, i.e., this step is a largely exothermic process for both 13BD geometries, demanding −0.68 eV and −0.55 eV for *cis*-2B and *trans*-2B products, respectively. Simultaneously, it is necessary

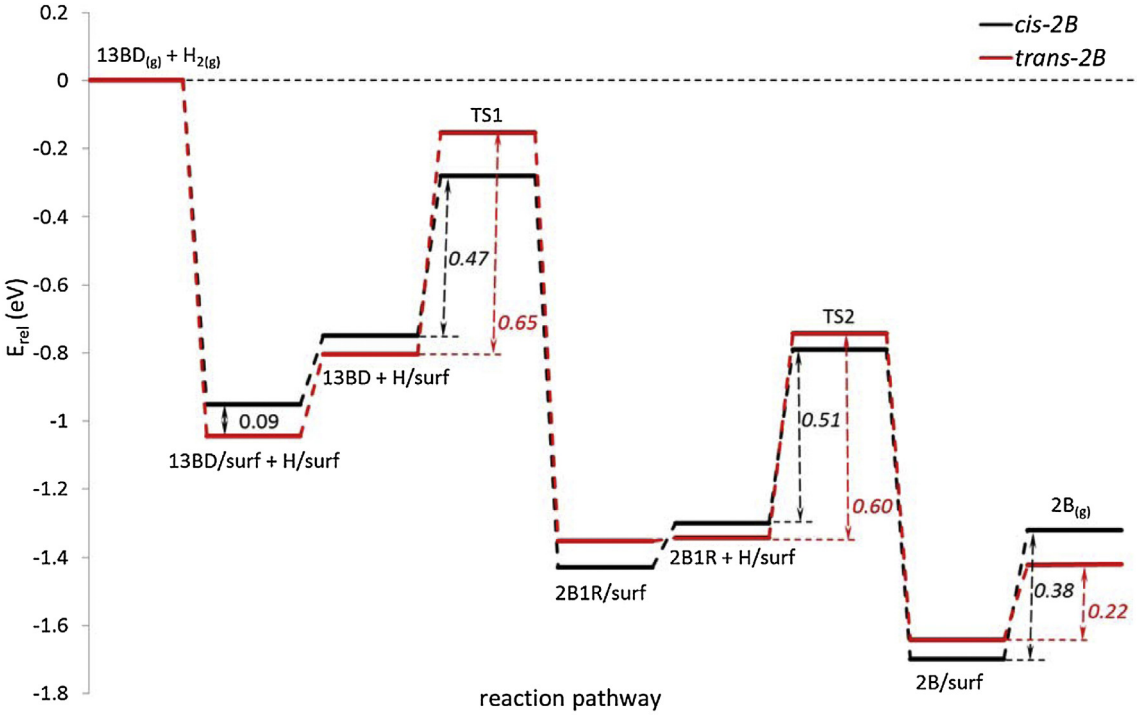

Fig. 4. 13BD hydrogenation energy profiles on Pd/Ni(1 1 1) following through 2B1R intermediate, to obtain *cis*- and *trans*-2B.

Table 3
Transition state barriers (ΔE_{TS}), in eV, and more relevant bond distances, in Å, of intermediates and H co-adsorbed species and TS geometries in the *trans*-2B to *cis*-2B isomerization on Pd/Ni(1 1 1) surface.

Species	ΔE_{TS}	Pd—H	C—H	Pd—C	C=C
trans-2B + H	–	1.83	2.97	2.15	1.45
TS1 (*trans*-2B + H → *trans*-2butyl)	0.98	1.59	1.83	2.78	1.43
trans-2butyl	–	2.37	1.11	3.26	1.52
TS2 (*trans*-2butyl → *cis*-2butyl)	0.10	2.23	1.11	3.23	1.52
cis-2butyl	–	2.86	1.10	3.59	1.52
TS3 (*cis*-2butyl → *cis*-2B + H)	1.16	1.59	1.83	2.86	1.43
cis-2B + H	–	1.87	2.47	2.17	1.44

to overpass the transition state barriers TS1 of 0.47 eV for *cis*-2B (see Fig. 3b) and 0.65 eV for *trans*-2B (see Fig. 2b), making kinetically more feasible the *cis*-2B production than the *trans*-2B isomer. In the next step of both reaction pathways the 2B1R intermediates are co-adsorbed with H atoms. While the *cis*-2B1R + H co-adsorption requires an amount of energy of 0.13 eV, the *trans*-2B1R + H co-adsorption is thermodynamically neutral. The production of butene from 2B1R is also an exothermic process but with an energy requirement of lower magnitude than the first hydrogenation one, demanding −0.40 eV and −0.31 eV for *cis*-2B and *trans*-2B pathways, respectively. Again, the transition state barrier TS2 to obtain *trans*-2B is slightly higher than for the *cis*-2B product (Fig. 2d and 3d, respectively). In other words, in spite of the fact that 13BD adsorbed on the di-π-*cis* site is 0.09 eV less stable than on the 1,2,3,4-tetra-σ site, the TS1 and TS2 transition state barriers are lower by 0.18 and 0.09 eV, respectively. Moreover, the *trans*-2B desorption is slightly favored with respect to the *cis*-2B.

In general, the experimental results scarcely evaluate the *cis*/*trans*-2B ratio and, in almost all the cases where this ratio is analyzed, its value is lower than the unit. This is valid for different catalysts, especially Pd- and Pt-based catalysts [11,47–51]. The production of a specific isomer can be useful to know which factors are essential in order to obtain the desired selectivity in partial hydrogenation reactions. Recently, Yang et al. [52] using combined experimental and theoretical investigations, found that gold catalysts have an unusual selectivity for 13BD hydrogenation toward *cis*-2B. In their theoretical approach, the di-π-*cis* and di-π-*trans* adsorption modes of 13BD on Au(1 1 1), Au(1 0 0) and Au_{19} cluster were evaluated. The calculations indicated that the di-π-*cis* mode was energetically more favorable than di-π-*trans* mode. These authors considered that this result explains the behavior experimentally observed.

From our present results we can conclude that once the 13BD is adsorbed on 1,2,3,4-tetra-σ or di-π-*cis* active sites of Pd/Ni(1 1 1), the hydrogenation reaction will produce *trans*-2B and *cis*-2B, respectively, with the latter isomer more favored than the first one. For this reason, the *cis*/*trans*-2B ratio would be increased on Pd/Ni(1 1 1), compared with the experimentally obtained result on Pd(1 1 1). This observation, valid for a low H precoverage, can be associated with experimental studies at low H pressure.

The comparison of theoretical results for the 13BD hydrogenation reaction produced on Pd/Ni(1 1 1) and Pd(1 1 1) surfaces could give us evidence about the role played by the lattice constants at surfaces. Despite that here this reaction was not evaluated on Pd(1 1 1) with the 13BD adsorbed in di-π-cis site, nevertheless we could to appeal to the results previously published work for the partial hydrogenation of 13BD adsorbed on 1,2,3,4-tetra-σ site, where a reaction barrier of 1.01 eV was obtained [23]. As it was outlined in the last work, the shortening of lattice parameter from Pd(1 1 1) to Pd/Ni(1 1 1), from 3.97 to 3.64 Å, produces the decrease of surface Pd—Pd interatomic distances from 2.82 to 2.57 Å [29,40]. The smaller interatomic distance on Pd/Ni(1 1 1) is compatible with a more stresses structure and a higher destabilization of 13BD, compared with Pd(1 1 1), and it is possible that for this reason the 13BD molecule is more activated on Pd/Ni(1 1 1) than on Pd(1 1 1) surface.

3.2. Trans-*2B*/cis-*2B isomerization*

In this section, the *cis*-2B isomer obtained from the *trans*-2B isomerization on Pd/Ni(1 1 1) is evaluated (Scheme 2) and the results are summarized in Table 3. In Figs. 5 and 6 are shown the corresponding optimized geometries of activated complexes and the energy profile, respectively.

In the TS1 geometry, from *trans*-2B + H co-adsorption to *trans*-2-butyl, the molecule is tilted toward the opposite side to the incoming H atom, preserving the CH_3—C=C angle (see Fig. 5a). The Pd—C bond is enlarged, while the Pd—H, C—H and C=C distances are shortened with respect to the previous reacting *trans*-2B and H co-adsorbed species. As it was observed for the H additions described in section 3.1, the Pd—H bond becomes shorter in comparison with the earlier species because the H atom gets closer to the Pd where the C atom is linked, while it moves away from the other two Pd atoms of the neighboring *fcc* hollow site. The increase of Pd—C distance is accompanied by a shortening of the C=C bond.

The *trans*-2-butyl clearly shows the stretching of the C=C double bond after the H addition into the secondary C atom. The C

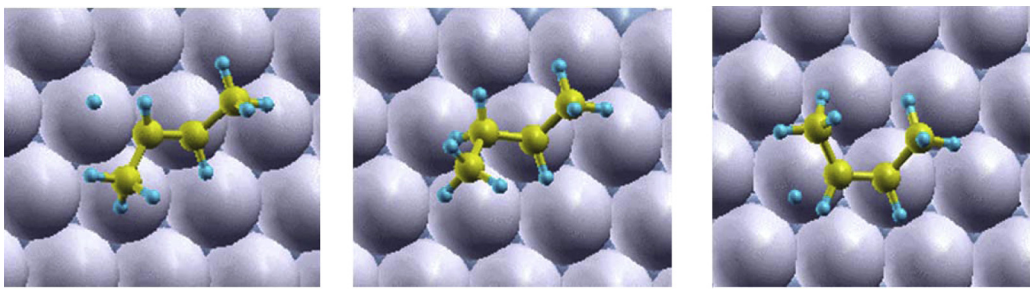

Fig. 5. Transition state structures of the *trans*-2B isomerization on Pd/Ni(1 1 1): (a) from *trans*-2B to *trans*-2butyl (TS1), (b) *trans*-2butyl to *cis*-2butyl (TS2) and (c) *cis*-2butyl to *cis*-2B (TS3).

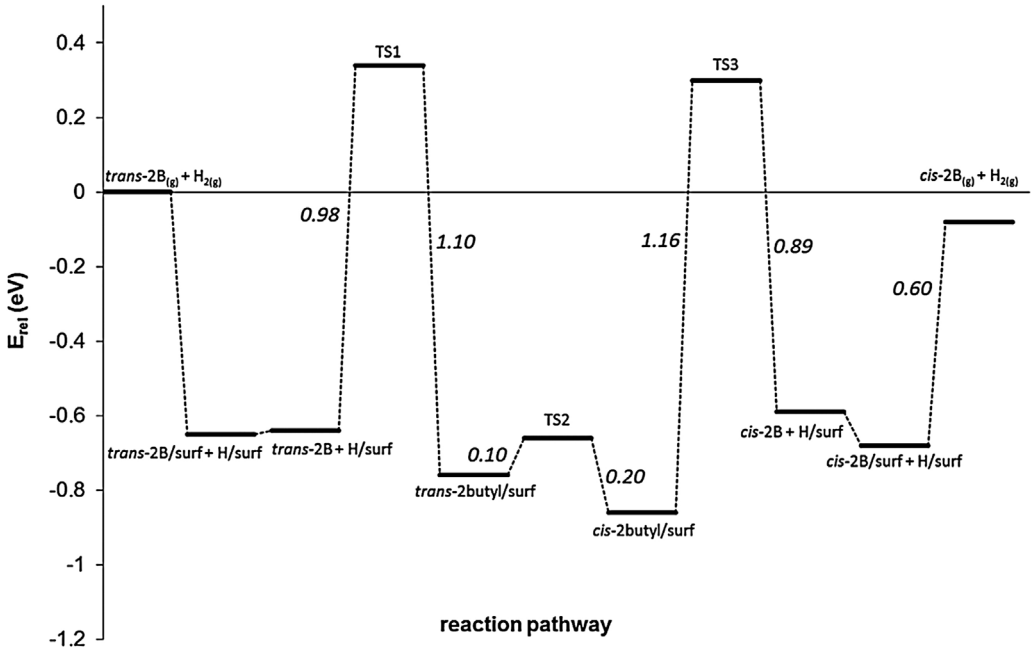

Fig. 6. *trans*-2B isomerization energy profile to obtain *cis*-2B on Pd/Ni(1 1 1).

hybridization changes from sp^2 to sp^3 giving a length of 1.52 Å for the C-C distance. In the TS2 geometry, from *trans*-2butyl to *cis*-2butyl species, the Pd-H distance is relatively short due to the rotation through the C—C central simple bond. In this situation, the H atom is pointing to the surface, while the methyl group is changing its position to the same side of the other methyl group (see Fig. 5b).

The TS3 geometry, which comprises the dehydrogenation of *cis*-2butyl intermediate, has similar distances than those reported in the TS1 geometry, excepting for the Pd—C bond (see Table 3). This bond is more elongated due to the tilting of whole species in the opposite direction to the incoming H atom, as well as the higher distance from the surface (Fig. 5c).

The energy profile shows that the formation of *trans*-2butyl intermediate needs 0.98 eV to overcome the TS1 (Fig. 5a), while the rotation of methyl group through the C—C central bond to obtain the *cis*-2butyl intermediate requires only 0.10 eV (TS2) (see Fig. 5b). Besides, *cis*-2butyl is 0.10 eV more stable than *trans*-2butyl species. Finally, the third step (TS3) barrier with 1.16 eV implies the most important energy requirement of the overall reaction (Fig. 5c). Notice that the greater energetic barriers correspond to the dehydrogenations of both butyl isomers: 1.10 and 1.16 eV for *trans*-2-butyl and *cis*-2butyl, respectively. In *cis*/*trans*-2B isomerization on Pd(1 1 1) [53], the energy barriers for *cis*/*trans*-2B partial hydrogenation are lower than on Pd/Ni(1 1 1) and the butyl intermediates have lower stabilities than on Pd/Ni(1 1 1), which leads to smaller barriers for the dehydrogenation step. The isomerization from *cis*-2B to *trans*-2B on Pd(1 1 1) is a more feasible process than on Pd/Ni(1 1 1).

In a recently work published by Li et al. [54], the *cis*/*trans* isomerization on Pt(1 1 1) was theoretically studied considering two hydrogen precoverages. At a H surface coverage of 0.11, the first activated energy barriers are similar than those obtained here (0.92 eV and 0.93 eV for *cis*-2B and *trans*-2B hydrogenation, respectively) and the butyl intermediate dehydrogenation requires also lower energy to form the *trans*-2B. Although the TS energy difference for the first hydrogenation is small, these authors considered that the isomerization from *cis*- to *trans*-2B isomers is an easier process than the inverse reaction and that the limiting step is the hydrogenation.

In our Pd/Ni(1 1 1) catalytic model, the isomerization from *cis*-2B to *trans*-2B is also a slightly more feasible reaction than the reverse process, with their hydrogenation barriers of 0.89 eV and 0.98 eV, respectively. In addition, the energy required to form *cis*-2B from the butyl isomer, 0.27 eV, is higher than that to form *trans*-2B, 0.12 eV, with the corresponding energy barriers of 1.16 eV and 1.10 eV, respectively. In this bimetallic surface the energy demanded for dehydrogenate the butyl isomers constitutes an energetic limitation due to the better stabilities of intermediates than the 2B isomers. Anyway, it is possible to conclude from these results that the geometric isomerization from *trans*-2B to *cis*-2B, and vice versa, requires a high energy cost to be overcome at low hydrogen coverage and that, for this reason, the reaction would be unlikely on this surface.

It is to be outlined, as it was previously mentioned by other authors, that the hydrogen coverage could change the isomerization mechanism and decrease the activation barriers [52,54]. In the present work, our interest is focused to study the competition of two possible mechanisms to obtain the *cis*-2B isomer on Pd/Ni(1 1 1) surface at low H coverage.

4. Conclusions

Two different reactions to produce *cis*-2B isomer on Pd/Ni(1 1 1) bimetallic surface by the direct hydrogenation of adsorbed 13BD on an appropriated *cis*-geometry site and by the isomerization of *trans*-2B were studied using periodic DFT calculations. In the first reaction, two competitive pathways produce *cis*-2B and *trans*-2B from the 13BD species adsorbed on di-π-*cis* and 1,2,3,4-tetra-σ active sites of Pd/Ni(1 1 1), respectively. The energetic profiles indicate the slightly favored *cis*-2B production, compared with the corresponding *trans*-species, especially in the first hydrogenation step. For this reason, an increase of the *cis*/*trans*-2B ratio on a Pd/Ni(1 1 1) catalyst, compared with the experimentally obtained on Pd(1 1 1), is expected.

The isomerization process from *trans*-2B to *cis*-2B could be feasible once the *trans*-2B isomer is formed. The hydrogenation energy barriers are almost twice the energy obtained in the first step of the hydrogenation reaction. The dehydrogenation barriers are even higher than the hydrogenation ones, because of the bigger stability

of partial hydrogenated 2-butyl intermediates than the dehydrogenated counterparts. For this reason, the geometric isomerization from *trans*-2B to *cis*-2B would be unlikely in this surface, in comparison with Pd(1 1 1) and Pt(1 1 1) surfaces.

The main conclusion of the presented results is that the *cis*-2B isomer would be produced on Pd/Ni(1 1 1) by the partial hydrogenation of 13BD adsorbed with appropriated *cis*-geometry site instead of the isomerization of *trans*-2B previously formed.

Acknowledgements

The authors thank the financial support from the Consejo Nacional de Investigaciones Científicas y Técnicas (CONICET), the Agencia de Promoción Científica y Tecnológica (ANPCyT) and the Universidad Nacional del Sur (UNS), under Grants PIP N°112-200801-02286, PICT-2010-0830, PGIs 24/F05 and 24F/055, respectively.

References

[1] G.C. Bond, P.B. Wells, Adv. Catal. 15 (1965) 91–226.
[2] J.R. Anderson, B.G. Baker, in: J.R. Anderson (Ed.), Chemisorption and Reactions on Metallic Films, vol. 2, Academic Press, London, 1971, p. 63.
[3] F. Zaera, Langmuir 12 (1996) 88–94.
[4] E.S. Jang, M.Y. Jung, D.B. Min, Compr. Rev. Food Sci. Food Saf. 4 (2005) 22–30.
[5] J.T. Judd, B.A. Clevidence, R.A. Muesing, J. Wittes, M.E. Sunkin, J.J. Podczasy, Am. J. Clin. Nutr. 59 (1994) 861–868.
[6] H. Arnold, F. Dobert, J. Gaube, in: G. Ertl, J. Weitkamp (Eds.), Handbook of Heterogeneous Catalysis, vol. 5, WILEY-VCH, Weinheim, 1997, p. 2165.
[7] J.C. Bertolini, J. Massardier, in: D.A. King, D.P. Woodruff (Eds.), The Chemical Physics of Solid Surfaces and Heterogeneous Catalysis, vol. 3B, Elsevier, Amsterdam, 1990, p. 107.
[8] J.C. Bertolini, A. Cassuto, Y. Jugnet, J. Massardier, B. Tardy, G. Tourillon, Surf. Sci. 349 (1996) 88–96.
[9] G. Tourillon, A. Cassuto, Y. Jugnet, J. Massardier, J.C. Bertolini, J. Chem. Soc., Faraday Trans. 92 (1996) 4835–4841.
[10] S. Katano, H.S. Kato, M. Kawai, K. Domen, J. Phys. Chem. B 107 (2003) 3671–3674.
[11] S. Katano, H.S. Kato, M. Kawai, K. Domen, J. Phys. Chem. C 112 (2008) 17219–17224.
[12] J. Massardier, J.C. Bertolini, J. Catal. 90 (1984) 358–361.
[13] M.P. Humbert, J.G. Chen, J. Catal. 257 (2008) 297–306.
[14] W. Yu, M.D. Porosoff, J.G. Chen, Chem. Rev. 112 (2012) 5780–5817.
[15] Y. Shu, L.E. Murillo, J.P. Bosco, W. Huang, A.I. Frenkel, J.G. Chen, Appl. Catal. A: Gen. 339 (2008) 169–179.
[16] J.R. Kitchin, J.K. Nørskov, M.A. Barteau, J.G. Chen, Phys. Rev. Lett. 93 (2004) 156801–156804.
[17] J. Arenas-Alatorre, A. Gómez-Cortés, M. Avalos-Borja, G. Diaz, J. Phys. Chem. B109 (2005) 2371–2376.
[18] N.A. Khan, M.B. Zeller, L.E. Murillo, J.C. Chen, Catal. Lett. 95 (2004) 1–6.
[19] S. Mc Ardle, J.J. Leahy, T. Curtin, D. Tanner, Appl. Catal. A: Gen. 474 (2014) 78–86.
[20] L. Porte, M. Phaner-Goutorbe, J.M. Guigner, J.C. Bertolini, Surf. Sci. 424 (1999) 262–270.
[21] R. Hou, W. Yu, M.D. Porosoff, J.G. Chen, T. Wang, J. Catal. 316 (2014) 1–10.
[22] G. Gómez, P.G. Belelli, G.F. Cabeza, N.J. Castellani, J. Mol. Catal. A: Chem. 394 (2014) 151–161.
[23] A. Valcárcel, A. Clotet, J.M. Ricart, F. Delbecq, P. Sautet, J. Phys. Chem. B 109 (2005) 14175–14182.
[24] W.W. Lonergan, X.J. Xing, R.Y. Zheng, S.T. Qi, B. Huang, J.G. Chen, Catal. Today 160 (2011) 61.
[25] A. Sarkany, Appl. Catal. A: Gen. 165 (1997) 87–101.
[26] J.W. Hightower, B. Furlong, A. Sarkany, L. Guczi, Stud. Surf. Sci. Catal. 75 (1993) 2305.
[27] H. Miura, M. Terasaka, K. Oki, T. Matsuda, Stud. Surf. Sci. Catal. 75 (1993) 2379–2382.
[28] N. El Kolli, L. Delannoy, C. Louis, J. Catal. 297 (2013) 79–92.
[29] A. Valcarcel, A. Clotet, J.M. Ricart, F. Delbecq, P. Sautet, Surf. Sci. 549 (2004) 121–133.
[30] F. Mittendorfer, C. Thomazeau, P. Raybaud, H. Toulhoat, J. Phys. Chem. B 107 (2003) 12287–12295.
[31] G. Gómez, P.G. Belelli, G.F. Cabeza, N.J. Castellani, J. Solid State Chem. 183 (2010) 3086–3092.
[32] G. Kresse, J. Hafner, Phys. Rev. B 47 (1993) 558–561.
[33] G. Kresse, J. Hafner, Phys. Rev. B 48 (1993) 13115–13118.
[34] G. Kresse, J. Hafner, Phys. Rev. B 49 (1994) 14251–14269.
[35] P. Blochl, Phys. Rev. B 50 (1994) 17953–18044.
[36] J.P. Perdew, J.A. Chevary, S.H. Vosko, K.A. Jackson, M.R. Pederson, D.J. Singh, C. Fiolhais, Phys. Rev. B 46 (1992) 6671–6687.
[37] J.P. Perdew, J.A. Chevary, S.H. Vosko, K.A. Jackson, M.R. Pederson, D.J. Singh, C. Fiolhais, Phys. Rev. B 48 (1993) 4978.
[38] H.J. Monkhorst, J.D. Pack, Phys. Rev. B 13 (1976) 5188–5192.
[39] M. Methfessel, A.T. Paxton, Phys. Rev. B 40 (1989) 3616–3621.
[40] G. Gómez, G.F. Cabeza, P.G. Belelli, J. Magn. Magn. Mater. 321 (2009) 3478–3482.
[41] H. Jónsson, G. Mills, in: J.B. Berne, G. Ciccotti, D.F. Coker, K.W. Jacobsen (Eds.), Classical and Quantum Dynamics in Condensed Phase Simulations, World Scientific, Singapore, 1998, p. 385.
[42] J. Horiuti, M. Polanyi, Trans. Faraday Soc. 30 (1934) 1164–1178.
[43] J. Horiuti, M. Polanyi, J. Mol. Catal. A: Chem. 199 (2003) 185–197.
[44] G.S. Hammond, J. Am. Chem. Soc. 77 (1955) 334–338.
[45] P.A. Sheth, M. Neurock, C.M. Smith, J. Phys. Chem. B 107 (2003) 2009–2017.
[46] M. Neurock, R.A. van Santen, J. Phys. Chem. B 104 (2000) 11127–11145.
[47] L.J. Shorthouse, Y. Jugnet, J.C. Bertolini, Catal. Today 70 (2001) 33–42.
[48] R.B. Moyes, P.B. Wells, J. Grant, N.Y. Salman, Appl. Catal. A: Gen. 229 (2002) 251–259.
[49] J. Silvestre-Albero, G. Rupprechter, H.-J. Freund, J. Catal. 235 (2005) 52–59.
[50] J. Silvestre-Albero, G. Rupprechter, H.-J. Freund, J. Catal. 240 (2006) 58–65.
[51] J. Silvestre-Albero, M. Borasio, G. Rupprechter, H.-J. Freund, Catal. Commun. 8 (2007) 292–298.
[52] X.-F. Yang, A.-Q. Wang, Y.-L. Wang, T. Zhang, J. Li, J. Phys. Chem. C 114 (2010) 3131–3139.
[53] P.G. Belelli, N.J. Castellani, Surf. Rev. Lett. 15 (2008) 249–259.
[54] J. Li, P. Fleurat-Lessard, F. Zaera, F. Delbecq, J. Catal. 311 (2014) 190–198.